

## Selective uptake of cesium by hybrid adsorbents enclosing heteropolyacid

Hitoshi Mimura, Shun Kanome, Yuichi Niibori

Graduate School of Engineering, Tohoku University, Japan

### Abstract

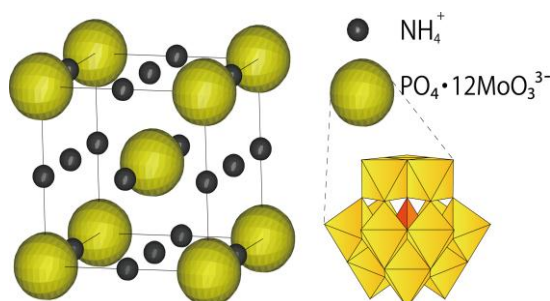
The selective separation and recovery of heat-generating nuclide ( $^{137}\text{Cs}$ ) from high-level liquid waste (HLLW) containing highly concentrated  $\text{HNO}_3$  and  $\text{NaNO}_3$  are vital issues in relation to the partitioning of radionuclides. Ammonium molybdophosphate [ $(\text{NH}_4)_3\text{PO}_4 \cdot 12\text{MoO}_3$ , AMP)], a fine crystal of heteropolyacid, with a high selectivity towards  $\text{Cs}^+$  ions, is one of the most promising adsorbents for this purpose. In order to granulate the fine AMP crystals, they can be incorporated into the macropores of zeolite (mordenite) by the sol-gel method using alginate gel polymer matrices. The present paper deals with the novel preparation methods for the hybrid adsorbents enclosing AMP fine crystals, their stability and the selective uptake properties for  $\text{Cs}^+$ . The mordenite enclosing AMP (AMP-M), a kind of inorganic/organic composite, was easily prepared by the successive impregnation of 1) PMA ( $\text{H}_3\text{Mo}_{12}\text{O}_{40}\text{P}$ ) and 2) kneaded sol [ $\text{NH}_4\text{NO}_3$  and sodium alginate (NaALG)] into the mordenite macropores. In this procedure, both synthesis and loading of AMP into the macropores are simultaneously accomplished. The synthetic reaction of AMP could be expressed as  $\text{H}_3\text{Mo}_{12}\text{O}_{40}\text{P} + 3\text{NH}_4\text{NO}_3 \leftrightarrow (\text{NH}_4)_3\text{PO}_4 \cdot 12\text{MoO}_3 + 3\text{HNO}_3$ , and the XRD intensities of AMP were almost constant up to the third loading run. Here the AMP-M composites obtained by 1<sup>st</sup> to 3<sup>rd</sup> cycles were abbreviated as AMP-M-1, -2 and -3, respectively. AMP-M composites were stable up to 200°C and had high uptake ability for  $\text{Cs}^+$  up to  $2.1 \times 10^7$  R irradiation ( $^{60}\text{Co}$ ). The uptake of  $\text{Cs}^+$  for AMP-M from  $\text{HNO}_3$  and  $\text{NaNO}_3$  solutions was examined by the batch method. The uptake of  $\text{Cs}^+$  for AMP-M in the presence of 0.01~5 M  $\text{HNO}_3$  attained equilibrium within 5 h, and a relatively large uptake percentage above 90% ( $K_d > 10^3 \text{ cm}^3/\text{g}$ ) was obtained; the uptake rate and uptake (%) of  $\text{Cs}^+$  for AMP-M were markedly enhanced compared to those for mordenite matrices. The AMP-M composites also exhibited relatively large  $K_d$  values above  $10^2 \text{ cm}^3/\text{g}$  for  $\text{Cs}^+$  even in the presence of 0.01~3M  $\text{NaNO}_3$ . The uptake ability of different metal ions for AMP-M was compared in the presence of 0.01~5 M  $\text{HNO}_3$ . The order of  $K_d$  value was  $\text{Cs}^+ \gg \text{Rb}^+ > \text{Ag}^+$ ; a significant difference was observed in  $K_d$  value between  $\text{Cs}^+$  and other cations. The maximum separation factors of  $\text{Cs}^+/\text{Rb}^+$  ( $K_{d,\text{Cs}}/K_{d,\text{Rb}}$ ) and  $\text{Cs}^+/\text{Ag}^+$  ( $K_{d,\text{Cs}}/K_{d,\text{Ag}}$ ) were estimated to be 23.9 and 100, respectively. The selective uptake (%) of  $\text{Cs}^+$  from simulated HLLW (SW-11E, 28 components, 2 M  $\text{HNO}_3$ , 1 M  $\text{NaNO}_3$ , JAEA) was estimated to be 70~80% for AMP-M-1~3.

*For practical use, the column adsorption properties (breakthrough and elution) were examined in the presence of 2.5 M HNO<sub>3</sub>. The breakthrough and total capacities were estimated to be 0.081 and 0.22 mmol/g from the symmetrical S-shaped curves, respectively. Further, the adsorbed Cs<sup>+</sup> on the AMP-M-3 column can be eluted by passing the eluent of 5 M NH<sub>4</sub>NO<sub>3</sub> solution and the elution (%) was estimated to be 95.4%. Thus, the AMP-M composites seem to be effective in the selective separation of Cs<sup>+</sup> ions from HLLW.*

## Introduction

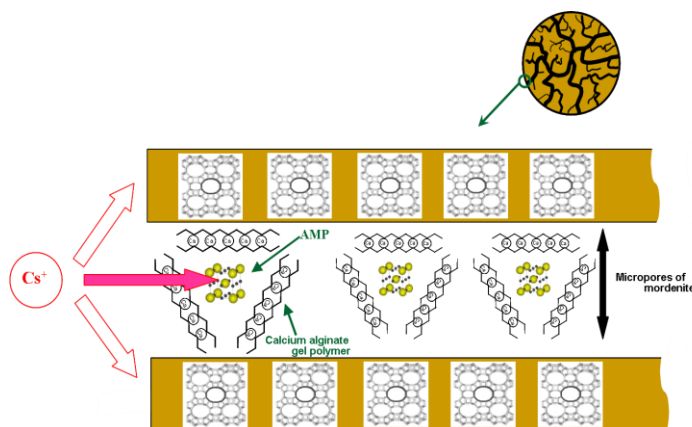
The selective separation and recovery of  $^{137}\text{Cs}$  from radioactive liquid wastes containing highly-concentrated  $\text{HNO}_3$  and  $\text{NaNO}_3$  have been of great interest in recent years for the application to volume reduction of radioactive wastes and partitioning of radionuclides [1] [2]. Ammonium molybdophosphate (AMP) with a high selectivity for  $\text{Cs}^+$  as shown in Figure 1, can act as one of the most promising inorganic ion-exchanger for this purpose [3] [4]. However, microcrystalline AMP exchanger is still not employed on a large scale because of its fine powder morphology which is unsuitable for the successive separation such as column operations. In order to overcome the handling problem, a mixture of AMP exchanger and asbestos was employed as a column bed [5], while this led to a marked lowering of bed density and uptake capacity.

**Figure 1: Chemical structure of AMP crystal with Keggin polyanions**



Mordenite is useful for column operations, because it can be granulated easily and has many macropores. Moreover, it has relatively high  $\text{Cs}^+$ -selectivity. By the loading of AMP crystals into macropores of mordenites, the enhancement of  $\text{Cs}^+$ -selectivity will be expected. In this study, calcium alginate gel polymer was used as immobilising matrices. Alginate gel polymer prevents the leakage of AMP fine crystals from the macropores of mordenites. The conceptual diagram of mordenite enclosing AMP microcapsules (AMP-M composite) is shown in Figure 2. The fine crystals of AMP and calcium alginate gel polymer are loaded into macropores of mordenite as AMP microcapsules. Both mordenites and AMP contribute to the uptake of  $\text{Cs}^+$  ions.

**Figure 2: Schematic diagram of AMP-M composites**



## Experimental

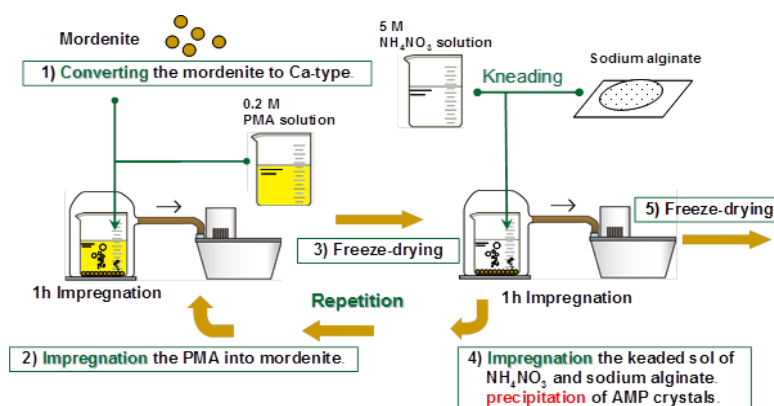
### Materials and preparation procedure of AMP-M

The synthesis of the mordenite enclosing AMP microcapsules (AMP-M) is as follows (Figure 3): First, three grammes of the mordenite (natural mordenite, Kawarago, Miyagi Pref.) were converted to Ca-type by conditioning with 5 M  $\text{Ca}(\text{NO}_3)_2$  (Wako Pure Chemical Ind.) solution. The Ca type of mordenite was dried at  $80^\circ\text{C}$ , and then added to  $25\text{ cm}^3$  of 0.2 M phosphomolybdic acid hydrate ( $\text{H}_3\text{Mo}_{12}\text{O}_{40}\text{P}$ ; Wako Pure Chemical Ind.; PMA) solution. The resulting solution was kept under reduced pressure and at room temperature for 1 h in order to impregnate the PMA into the mordenite macropores. The excess PMA solution was removed by filtration. The product was freeze-dried to impregnate PMA in the macropores of mordenite. In a similar manner, mordenites impregnating PMA were then treated with  $25\text{ cm}^3$  of kneaded sol of  $\text{NH}_4\text{NO}_3$  and sodium alginate (NaALG, 80-120 cP; Wako Pure Chemical Ind.) for the synthesis of AMP crystals. This synthetic reaction of AMP can be expressed as follows:



After freeze-drying, the product was sieved using a  $150\ \mu\text{m}$  sieve to remove fine AMP particles and finally stored in a sealed vessel. AMP-M composites obtained by the repeated impregnation (up to three times) were abbreviated as AMP-M1, AMP-M2 and AMP-M3, respectively.

**Figure 3: Preparation procedure of AMP-M composites**



### Characterisation of AMP-M

The structure of fine AMP crystals was checked by powder X-ray diffractometry (XRD, Rigaku MiniFlex) using monochromatised  $\text{Cu-K}\alpha$  radiation. The surface morphology and chemical composition were analysed by scanning electron microscopy (SEM, Hitachi Miniscope TM-1000) equipped EDS system. The thermal decomposition was examined by infrared absorption spectrometry (FT-IR, Horiba, FT-200) and thermogravimetry-differential thermal analysis (TG-DTA, Rigaku, TG8120).

### Determination of distribution coefficient

The distribution coefficients of various metal ions were determined by the batch method. An aqueous solution ( $4\text{ cm}^3$ ) containing 10 ppm metal ions were contacted with

0.040 g of adsorbents (mordenites, AMP-M1, AMP-M2 and AMP-M3) at  $25\pm 1^\circ\text{C}$  for 24 h, which was found to be sufficient for attaining equilibrium. In advance, a simulated high-level liquid waste (abbreviated as SHLLW, 28 components solution, SW-11E, JAEA) was also used, and the uptake of different metal ions was determined. After equilibration, the concentration of  $\text{Cs}^+$  ions in supernatant was measured by the atomic absorption spectrometer (Jarrel–Ash, AA-890), and that of other metal ions by ICP-AES (SII, SPS 7800). The uptake (%) of metal ions removed from the solution,  $R$  (%), and the distribution coefficient,  $K_d$  ( $\text{cm}^3/\text{g}$ ), are defined as;

$$R = [(C_i - C_t)/C_i] \times 100 \text{ (\%)}, \quad (2)$$

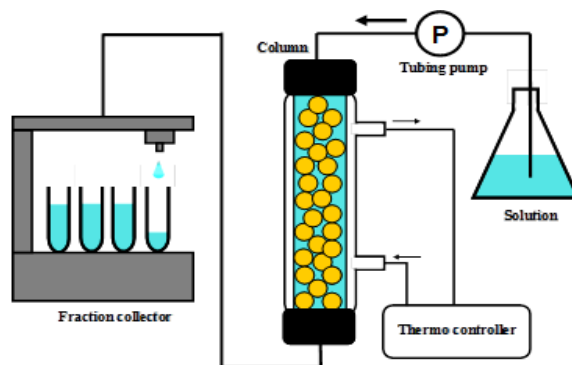
$$K_d = [(C_i - C_f)/C_f] \times V/m \text{ (cm}^3/\text{g)}, \quad (3)$$

where  $C_i$ ,  $C_t$ , and  $C_f$  (ppm) are the concentration at the initial stage, at time  $t$ , and at equilibrium, respectively;  $m$  (g) is the weight of the adsorbents; and  $V$  ( $\text{cm}^3$ ) is the volume of the aqueous phase.

### Breakthrough and elution tests

Two grammes of AMP-M3 composite were packed into the glass column ( $5 \text{ mm}\phi \times 200 \text{ mm}$  long) with a jacket thermostated at  $25\pm 1^\circ\text{C}$  (Figure 4). A breakthrough curve was obtained by plotting the breakthrough ratio ( $C/C_0$ ) against the effluent volume, where  $C_0$  and  $C$  (ppm) are the concentration of the initial feed solution and the effluent, respectively. Elution and regeneration of the column were carried out by passing the eluent of 5 M  $\text{NH}_4\text{NO}_3$  and 1 M  $\text{HNO}_3$ . An elution curve was obtained by plotting the elution(%) [% ratio of the amount of eluted metal ions to that of initial loaded ones] against the eluent volume.

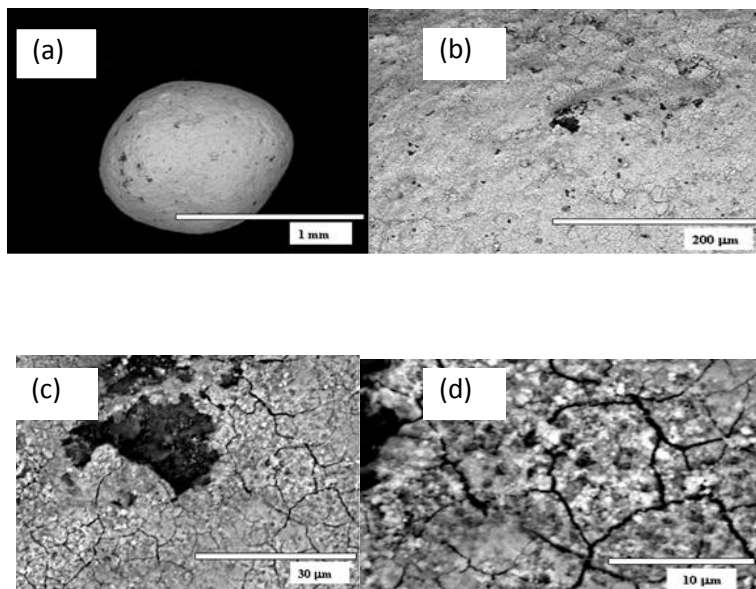
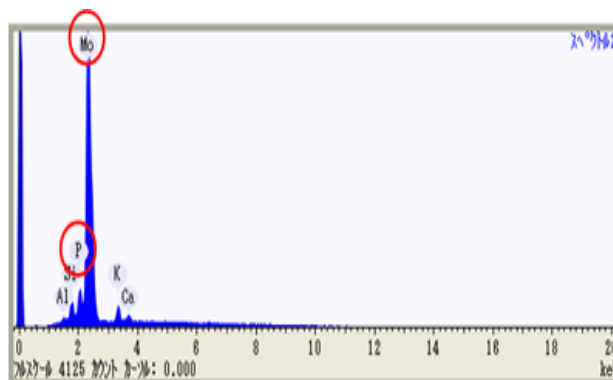
Figure 4: Apparatus for column experiments



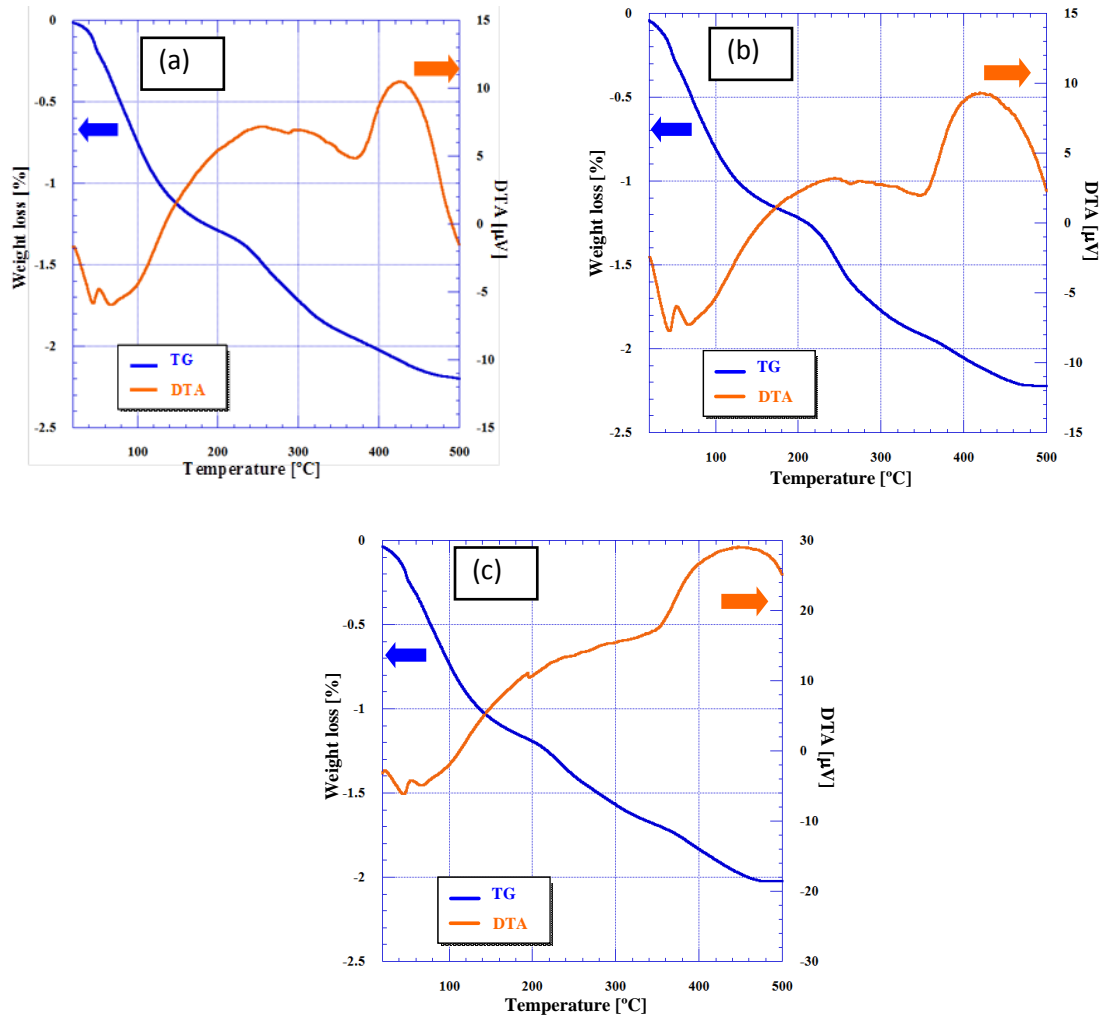
## Results and discussion

### Surface morphology and thermal stability

The fine powders of AMP with high  $\text{Cs}^+$ -selectivity were loaded into the macropores of mordenite using the calcium alginate gel polymer as immobilising matrices. The typical SEM images of AMP-M3 and the magnification of its surface are shown in Figures 5(a)–(d). In Figure 5(d), the aggregates of AMP crystals are observed on the surface of AMP-M3 composite; EDS for the cross-section of AMP-M3 composite shows the uniform distribution of Mo and P (Figure 6).

**Figure 5: SEM images of AMP-M3****Figure 6: EDS spectra of AMP-M3**

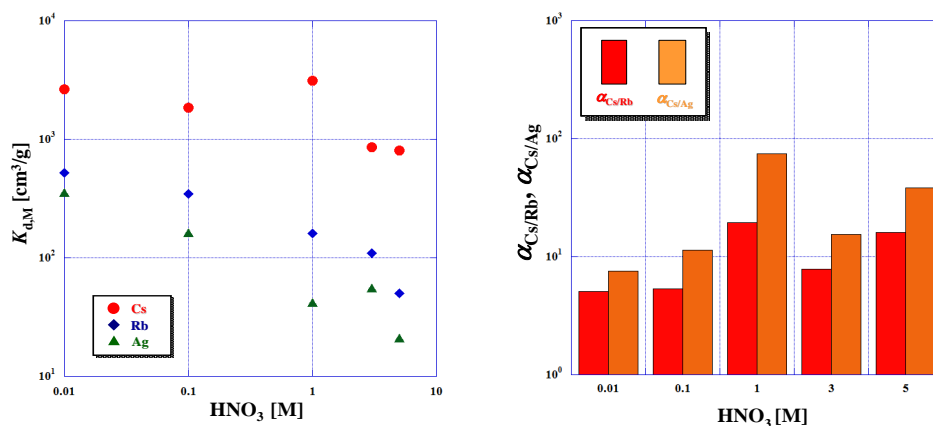
The thermal stability of AMP-M1, AMP-M2 and AMP-M3 composites was evaluated by TG/DTA analyses in the temperature range of 20°~500°C at heating rate of 5 K/min in N<sub>2</sub> atmosphere [Figures 7(a) ~ (c)]. Thermal changes were observed in three steps; the weight loss of adsorbed water up to around 100°C, the thermal decomposition of carboxyl ions (COO<sup>-</sup>) around 200°C, and the thermal decomposition of AMP crystal structure around 400°C. These findings suggest that the thermal stability of AMP-M composites can be maintained up to 200°C.

**Figure 7: TG/DTA curves of AMP-M1(a), AMP-M2(b) and AMP-M3(c) composites**

### Effects of $\text{HNO}_3$ concentration on $K_{d,\text{Cs}}$ and separation factor of Cs/Rb and Cs/Ag

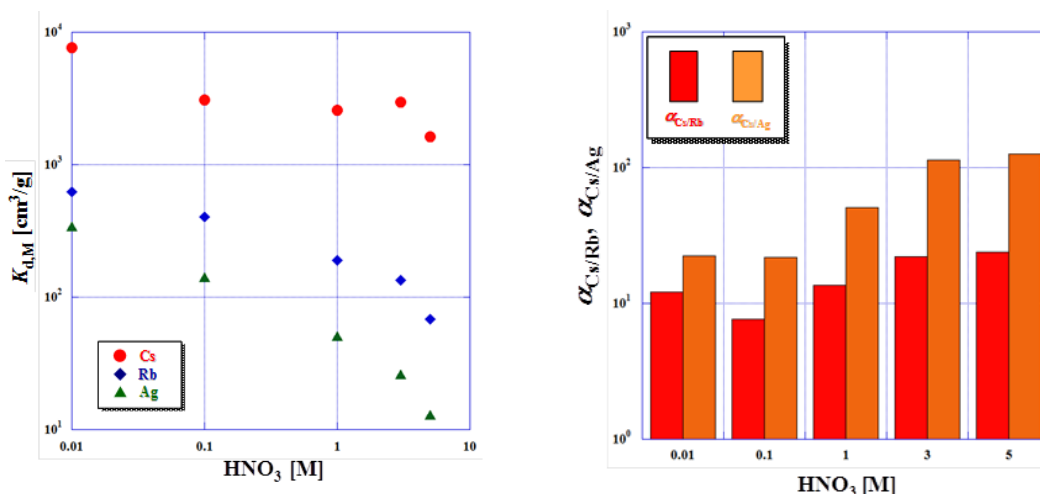
The effects of  $\text{HNO}_3$  concentration on  $K_d$  values of  $\text{Cs}^+$ ,  $\text{Rb}^+$  and  $\text{Ag}^+$  ions and the separation factor ( $\alpha_{\text{Cs/Rb}} = K_{d,\text{Cs}}/K_{d,\text{Rb}}$  and  $\alpha_{\text{Cs/Ag}} = K_{d,\text{Cs}}/K_{d,\text{Ag}}$ ) for AMP-M2 and AMP-M3 composites are shown in Figures 8 (a) and (b) and Figures 9(a) and (b), respectively. In either case, the  $K_{d,\text{Cs}}$  values were almost constant and estimated above  $10^3 \text{ cm}^3/\text{g}$  even in the presence of 1 M  $\text{HNO}_3$ . In contrast, the  $K_d$  values of  $\text{Rb}^+$  and  $\text{Ag}^+$  tended to decrease with  $\text{HNO}_3$  concentration. The estimated separation factors of  $\alpha_{\text{Cs/Rb}}$  and  $\alpha_{\text{Cs/Ag}}$  tended to increase with  $\text{HNO}_3$  concentration. Especially, relatively large separation factor of 23.9 was obtained for AMP-3M, suggesting the selective separation of  $\text{Cs}^+$  from HLLW (Figure 9).

**Figure 8: Effect of HNO<sub>3</sub> concentration on K<sub>d</sub> for AMP-M2 (left) and separation factor of Cs/Rb and Cs/Ag (right)**



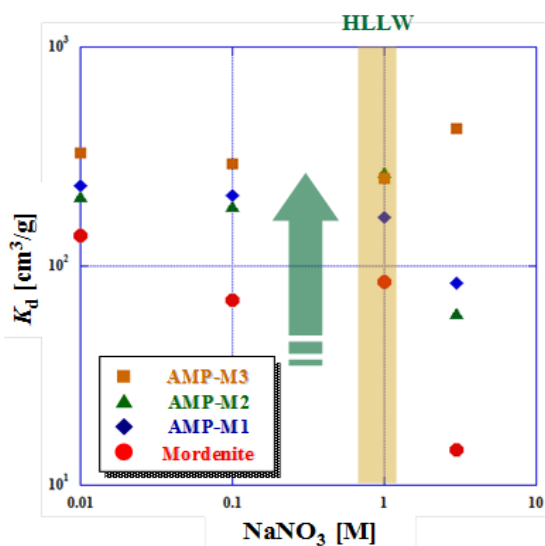
$V/m = 100 \text{ cm}^3/\text{g}$ ;  $[\text{Cs}^+] = 10 \text{ ppm}$ ;  $[\text{HNO}_3] = 0.01\text{-}5 \text{ M}$ ;  $25^\circ\text{C}$ ;  $24 \text{ h}$ .

**Figure 9: Effect of HNO<sub>3</sub> concentration on K<sub>d</sub> for AMP-M3 (left) and separation factor of Cs/Rb and Cs/Ag (right)**



### Effect of NaNO<sub>3</sub> concentration on K<sub>d,Cs</sub>

In the case of Cs separation from HLLW, the effect of NaNO<sub>3</sub> concentration on  $K_{d,Cs}$  should be estimated in advance. Figure 10 shows the effects of NaNO<sub>3</sub> concentration on  $K_{d,Cs}$  for AMP-M composites and mordenite matrix. The  $K_{d,Cs}$  values for AMP-M composites are larger than that of mordenite matrix, indicating the high selectivity of AMP towards Cs<sup>+</sup> ions. The order of  $K_d$  value was AMP-M3>AMP-M2>AMP-M1>>mordenite matrix; the AMP-M with higher AMP content tends to have a larger  $K_{d,Cs}$  value. The  $K_{d,Cs}$  values for AMP-M2 and AMP-M3 were estimated to be over 10<sup>2</sup> cm<sup>3</sup>/g in the presence of 1 M NaNO<sub>3</sub> which corresponds to the Na<sup>+</sup> concentration in HLLW.

**Figure 10: Effects of NaNO<sub>3</sub> concentration on  $K_{d,Cs}$  for AMP-M composites and mordenite matrix**

$V/m = 100 \text{ cm}^3/\text{g}$ ;  $[\text{Cs}^+] = 10 \text{ ppm}$ ;  $[\text{NaNO}_3] = 0.01\text{-}3 \text{ M}$ ;  $25^\circ\text{C}$ ;  $24 \text{ h}$ .

### Selective separation of Cs from simulated HLLW

Selective separation of Cs<sup>+</sup> in simulated HLLW (SHLLW, 28 components solution, SW-11E, JAEA) was examined using AMP-M composites. Figure 11 shows the uptake (%) of different elements in SHLLW for AMP-M composites. The uptake (%) of Cs<sup>+</sup>, Rb<sup>+</sup> and Ag<sup>+</sup> was estimated to be about 80, 30 and 10%, respectively, indicating the necessity of chromatographic separation. Relatively low uptake (%) of Ba, Ru, Rh and Eu, etc. was also obtained; the adsorption of these metal ions was due to the incorporation into alginate phase in composites. In advance, the removal of these metal cations by alginate seems to be essential for the effective separation of Cs<sup>+</sup>. After batch experiments, the formation of precipitates was observed in the reaction tubes and the precipitate contained Zr, Te and Se.

### Radiation stability

The estimation of radiation stability is important for the practical use of AMP-M composites in the separation process of actual HLLW. As for the radiation stability test, AMP-M1 composites were irradiated by <sup>60</sup>Co- $\gamma$  ray up to  $2.12 \times 10^7 \text{ R}$  (Tohoku University, <sup>60</sup>Co irradiation facility), and the uptake ability of Cs<sup>+</sup> for the irradiated specimens was estimated by the batch method. There is no appreciable alteration on the surface of the irradiated specimens of AMP-M1 before and after irradiation of <sup>60</sup>Co- $\gamma$  rays at  $2.12 \times 10^7 \text{ R}$  [Figures 12(a) and (b)]. Figure 13 shows the effect of <sup>60</sup>Co exposure on  $K_{d,Cs}$  for AMP-M1 composites. The  $K_{d,Cs}$  values were almost constant and a relatively large  $K_{d,Cs}$  value exceeding  $10^2 \text{ cm}^3/\text{g}$  was obtained even after irradiation at  $2.12 \times 10^7 \text{ R}$ .

Figure 11: Uptake (%) of different elements in SHLLW for AMP-M composites at  $V/m = 10 \text{ cm}^3/\text{g}$

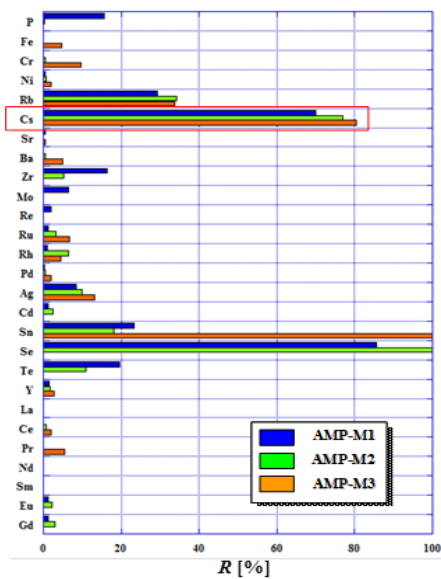


Figure 12: SEM images of the surface of AMP-M1 before (left) and after (right) irradiation of  $^{60}\text{Co}$ - $\gamma$  ray

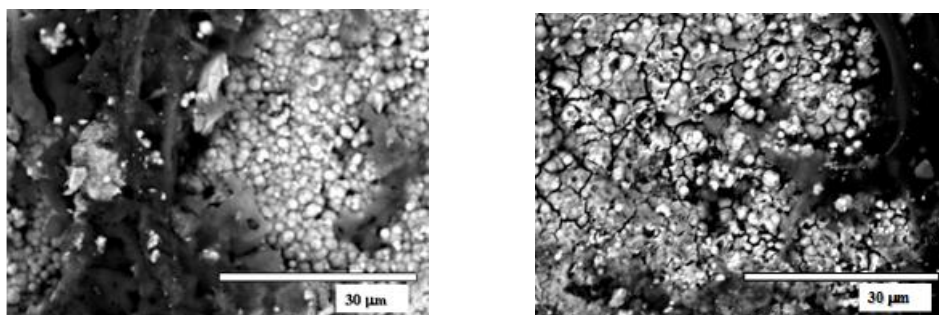
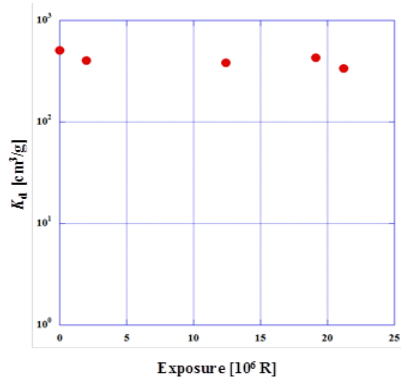


Figure 13: Effect of  $^{60}\text{Co}$  exposure on  $K_{d,Cs}$  for AMP-M1 composites

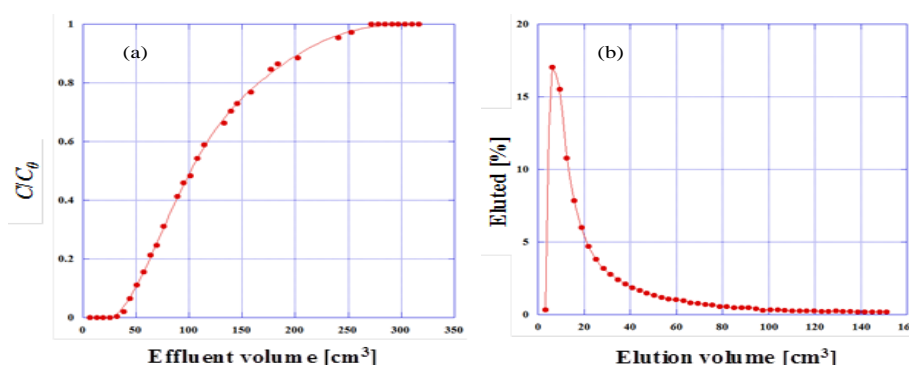


$V/m = 100 \text{ cm}^3/\text{g}$ ;  $[\text{Cs}^+] = 10 \text{ ppm}$ ;  $[\text{HNO}_3] = 3 \text{ M}$ ;  $25^\circ\text{C}$ ; 5 h.

### Breakthrough and elution properties of Cs<sup>+</sup> through AMP-M3 column

Figures 14(a) and (b) illustrate the breakthrough and elution curves of Cs<sup>+</sup> for the AMP-M3 column. The breakthrough curve had a symmetrical S-shaped profile, suggesting no dislodgement of AMP from the matrix of mordenite. The breakpoint of 5% breakthrough was estimated to be 42 cm<sup>3</sup>. The breakthrough capacity (B. T. Cap.) and total capacity (T. Cap.) were calculated to be 0.081 and 0.22 meq/g, respectively. The column packed with AMP-M composites was thus effective for the selective removal of Cs<sup>+</sup>. Further, the adsorbed Cs<sup>+</sup> on the column can be eluted by passing the eluent of NH<sub>4</sub>NO<sub>3</sub> solution, as shown in Figure 14(b). The elution (%) of Cs<sup>+</sup> adsorbing on the column was estimated to be 95%. The AMP-M composite column was regenerated after the elution with NH<sub>4</sub>NO<sub>3</sub>.

**Figure 14: Breakthrough (a) and elution (b) curves of Cs<sup>+</sup> for AMP-M3 column**



Column: 0.5 cm $\phi$ ×20 cm, AMP-M3: 2 g; flow rate: 0.23-0.25 cm<sup>3</sup>/min; 25°C;  
feed solution: [Cs<sup>+</sup>] = 500 ppm, 2.5 M HNO<sub>3</sub>; eluent: 5 M NH<sub>4</sub>NO<sub>3</sub>/ 1 M HNO<sub>3</sub>.

### Conclusions

The mordenite enclosing AMP (AMP-M), a kind of inorganic/organic composites, was easily prepared by the successive impregnation of 1) PMA (H<sub>3</sub>Mo<sub>12</sub>O<sub>40</sub>P) and 2) kneaded sol of NH<sub>4</sub>NO<sub>3</sub> and sodium alginate (NaALG) into the mordenite macropores. In this procedure, both synthesis and loading of AMP crystals into the macropores are simultaneously accomplished. The uptake ability of different metal ions for AMP-M was compared in the presence of 0.01~5 M HNO<sub>3</sub>. The order of  $K_d$  value was Cs<sup>+</sup> >> Rb<sup>+</sup> > Ag<sup>+</sup>. The maximum separation factors of Cs/Rb ( $K_{d,Cs}/K_{d,Rb}$ ) and Cs/Ag ( $K_{d,Cs}/K_{d,Ag}$ ) were estimated to be 23.9 and 100, respectively. As for simulated HLLW, relatively large uptake (%) of Cs<sup>+</sup> about 70~80% was obtained for AMP-M1~3. The breakthrough and total capacities were estimated to be 0.081 and 0.22 mmol/g from the symmetrical S-shaped curve, respectively. Further, the adsorbed Cs<sup>+</sup> on the AMP-M3 column can be eluted by passing the eluent of 5 M NH<sub>4</sub>NO<sub>3</sub> solution and the elution (%) was estimated to be 95.4%. Thus, the AMP-M composites are effective for the selective separation of Cs<sup>+</sup> ions from HLLW.

## References

- [1] IAEA Technical Rep. Ser., No. 356, IAEA, Vienna, (1993).
- [2] M. Kubota et al. (1998), *Proc. Fifth Int. Information Exchange Meeting on Actinide and Fission Product Partitioning and Transmutation*, OECD/NEA, Paris, 131.
- [3] V. Pekarek, V. Vesely (1972), *Talanta*, 19, 1245–1248.
- [4] M. Qureshi, K. G. Varshney (1991), *Inorganic Ion Exchangers in Chemical Analysis*, CRC Press Inc., Boston, 57–90.
- [5] J. van R. Smit, W. Robb, J. J. Jacobs, J. Inorg (1959), *Nucl. Chem.*, 12, 104.